Journal of Ceramic Processing Research. Vol. 14, No.2, pp. 188~193 (2013)

J O U R N A L O F
Ceramic Processing Research

Study on change of electrical properties of ZnO thin films deposited in low temperature facing targets magnetron sputtering (FTS) system with H_2 and O_2 flow rate changes

Hye R. Kim*, Su B. Jin, Long Wen, Yoon S. Choi, In S. Choi, M. Hori and Jeon G. Han

NU-SKKU Joint Institute for Plasma-Nano Materials, Sungkyunkwan University, 300 Chunchun-dong, Jangan-gu, Suwon 440-746, Republic of Korea

The optical, structural and electrical properties of ZnO thin film deposited by FTS system with H_2 and O_2 addition at low processing temperature were studied. The sheet resistance of the ZnO thin film increased from ~10^{-3} to ~10^{6} Mohm/sq. with the O_2 flow rate and decreased from ~10^{-1} to ~10^{-4} Mohm/sq. with the H_2 flow rate increase. The increase of sheet resistance with O_2 flow rates could be explained by oxygen vacancies. The decrease of sheet resistance with H_2 flow rates could be explained by increase of the electrons from interstitial hydrogen atoms. The electrical property showed dramatic change with the small change of the flow rates. Conversely, the optical and structural characteristics did not show large variation. According to H_2 and O_2 flow rate change, transmittance of the deposited ZnO thin film varied in the range of 84 ~ 87% while the optical band gap showed small shift to the range of 3.22 eV ~ 3.26 eV. XRD measurements showed that the deposited ZnO thin film was composed of amorphous and crystalline phase and the grain size varied in the range of 15.37 ~ 17.89 with the flow rate change of H_2 and O_2. The plasma characteristics were analyzed using optical emission spectroscopy (OES) but the overall spectrum did not change with the H_2 and O_2 gas flow rates. Therefore, the dramatic changes in the electrical properties of ZnO thin films could be attributed to change in chemical composition of the thin films rather than the plasma status.

Key words: ZnO thin film, Facing targets magnetron sputtering (FTS), Low temperature process, Sheet resistance, Optical band gap.

Introduction

ZnO has been studied for various applications including gas sensors [1], transducers [2], heaters and defrosters [3], solar cells [4], diluted magnetic semiconductors (DMS) [5], and electronic and optoelectronic devices such as ultraviolet photodetectors [6], light-emitting diodes (LED) [7], surface acoustic wave (SAW) devices [8], and transparent electrodes [9, 10]. Due to a direct wide band gap of 3.36 eV and large exciton binging energy (60 meV), ZnO was used in a wide range of electronic and optical applications. Other merits of high oxidation ability, high sensitivity to many gases and low costs were considered in application of gas sensors and photocatalyst [11-15].

However, the origin of n-doping in Al-doped ZnO has long been debated and not clearly understood, and moreover, the electrical properties of the currently developed ZnO are insufficient to replace ITO. In recently published papers, hydrogen has been highlighted due to its role in n-doping and defect passivation, theoretically and experimentally. Traditionally, oxygen vacancies have been known to be a major contributor to n-doping similar to ITO. But in the case of ZnO, careful calculation has revealed that oxygen vacancies are in deep donor state with little contribution to n-doping [11]. On the other hand, it was recently shown that hydrogen can substitute the oxygen vacancy sites and release one electron constituting a shallow donor state, or constitute interstitial sites in the vicinity of Zn vacancies as a shallow donor as well [16].

We reported characteristics of ZnO thin films deposited at the upper substrate position of FTS system with H_2 and O_2 flow rate change [25]. In this study, ZnO thin films were deposited at the down substrate position of FTS system with H_2 and O_2 flow rate change and investigated the changes in optical, structural and electrical ZnO thin film properties.

Experimental details

The schematic of the experimental setup is shown in Fig. 1. The FTS system was installed inside a cylindrical vacuum chamber of 700 mm length and 490 mm inner diameter. The system is composed of two facing ZnO target electrodes, 250 mm × 100 mm in size with a gap of 70 mm to which pulsed DC power was applied. During all experiments, the pulsed DC power was fixed at 700 W. On the rear side of the ZnO target electrodes were attached a number of magnets which form the magnetic field distribution directing from one target surface to the other. The base pressure and working pressure were 5×10^{-6} Torr and 5×10^{-3} Torr, respectively. An $Ar/H_2/O_2$ gas mixture was injected into the FTS system through small holes formed on a square gas

*Corresponding author:
Tel : +82-31-290-5666
Fax: +82-31-290-5669
E-mail: nanoplasma@skku.edu

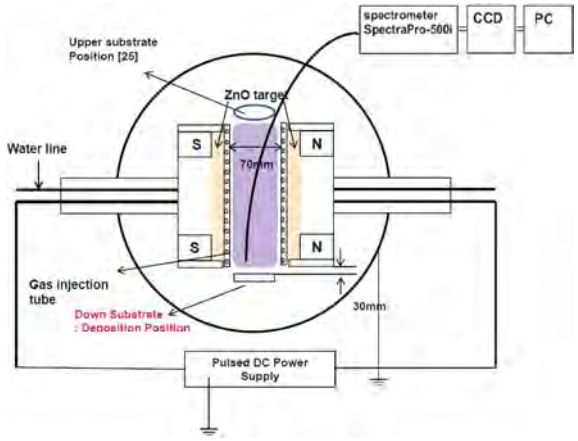

Fig. 1. Schematic diagram of the Facing targets sputtering (FTS) system used to deposit the ZnO thin films.

Table 1. The deposition process parameters used to deposit ZnO thin Film.

Parameters	Conditions
Target	ZnO
Base pressure	Below 5×10^{-6} Torr
Deposition pressure	5×10^{-3} Torr
Ar gas	177 sccm
O_2 gas	0.2 ~ 1 sccm
H_2 gas	0.2 ~ 1 sccm
Power (Pulsed dc)	700 W
Frequency	150 kHz, 2.9 μs
Substrate	Glass
Distance $_{E\text{-}E}$	70 mm
Top distance $_{E\text{-}S}$	30 mm
Substrate temp.	Room temperature

tube in front of ZnO targets.

A glass substrate 75 mm × 20 mm in size was placed below the facing target electrodes - down substrate position - by attaching it to a metallic plate. Compared to upper position [25], substrate position was close to pumping port. This would infer to different effect of gas molecules to the deposition of ZnO thin film. The distance between the bottom edge of the facing targets and the substrate was 30 mm. The substrate temperature was kept at room temperature before deposition of ZnO thin film. The deposition time was 270 seconds. During the deposition, the substrate temperature was measured using a thermocouple. The ion current density to which the substrate would be exposed was measured through separate insertions of copper plates for the respective process conditions.

The process parameters used to deposit the ZnO thin film are listed in Table 1. The flow rates of H_2 and O_2 gases were changed separately. The thickness of deposited ZnO thin films was about 150 nm by α-step.

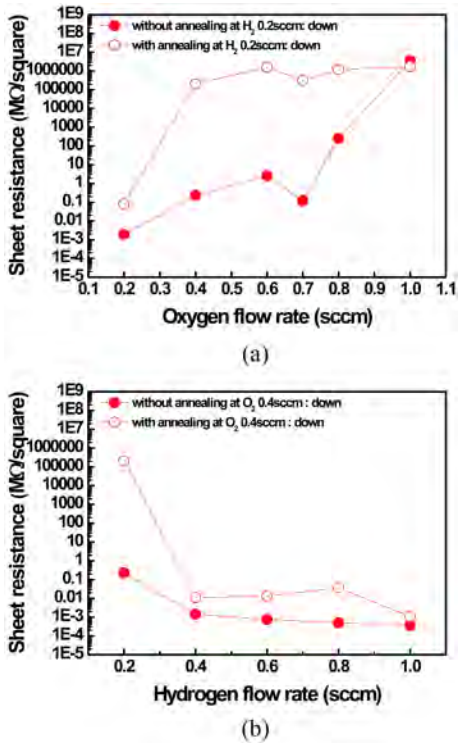

Fig. 2. Sheet resistance of ZnO thin film with and without annealing treatment according to (a) O_2 and (b) H_2 gas flow rates change, respectively.

The ZnO thin films were annealed for 60 min at 100 ºC in a separate annealing chamber under atmospheric environment.

The optical properties of the ZnO thin films were studied by UV-VIS-NIR spectrometer (Shimadzu, ISR-3100) in the wavelength range of 200 nm - 1000 nm. The electrical properties of the ZnO thin films were measured with a sheet resistance meter. OES measurement was performed using a single fiber optic probe connected to a SpectraPro 500i spectrometer with a 100-um entrance slit of 200 nm to 900 nm range, and an Acton PIXIS 400 CCD camera with the sensor cooled to ~20.5 ºC during deposition to analyze the chemical species affecting the reaction on the substrate.

Results and discussion

Electrical properties of ZnO thin films

Fig. 2 shows that the sheet resistance of ZnO thin film is closely related to O_2 and H_2 gas flow rate change. In Fig. 2(a), as O_2 gas flow rate increased from 0.2 sccm to 1.0 sccm, the sheet resistance increased from ~10^{-3} to ~10^{6} Mohm/sq without annealing. The slight increase of O_2 gas flow rates resulted in decrease of oxygen vacancies in the ZnO thin films, and the sheet resistance increased dramatically. In comparison with ZnO thin film deposited at upper position [25], deposition at down position showed few order of magnitude higher sheet resistance. As the pumping port

is close at the down position, supply of more O atoms at the down position than upper position can be attributed to the increase of sheet resistance. The annealing treatment resulted in increase of sheet resistance. This change of sheet resistance with annealing could be attributed to the O_2 intrusion into the ZnO thin film during the annealing in an atmospheric environment and subsequent decrease in oxygen vacancies.

Fig. 2(b) shows that as H_2 gas flow rate increased from 0.2 sccm to 1.0 sccm, the sheet resistance decreased from ~10^{-1} to ~10^{-4} Mohm/sq without annealing treatment. The hydrogen in ZnO thin film becomes interstitial and substitutional hydrogen behaving as a shallow donor. As the density of substitutional hydrogen (H_o) or hydrogen interstitials (H_i) is low, the conductivity of the ZnO thin film decreases under O-rich conditions [21]. Whereas, n-doping is possible since hydrogen can substitute for oxygen vacancy (V_o) and release one electron, acting as a shallow donor under O-poor condition, so the conductivity increases. As H_o remains stable state until 500 °C, the sheet resistance increases for H_i diffusing out during annealing [21]. The annealing treatment resulted in increase of the sheet resistance, which is a similar trend to the case increase of O_2.

Optical properties of ZnO thin films

Fig. 3(a) showed the transmission spectra for the ZnO films deposited with various flow rates of the H_2 gas. The transmittance is over 86% in the visible region for all the samples. As seen from Fig. 3(a), the absorption tails near 280 nm are present.

The absorption coefficient α can be calculated from the relation [20]:

$$T = A \exp(-\alpha d) \quad (1)$$

where T is the transmittance of thin film, A is a constant and approximately unity as the reflectivity is negligible and insignificant near the absorption edge, and d is the film thickness. The optical band gap of the film is determined by applying the Tauc model [21], and the Davis and Mott model [22] in the high absorbance region:

$$\alpha h\nu = D(h\nu - E_g)^n \quad (2)$$

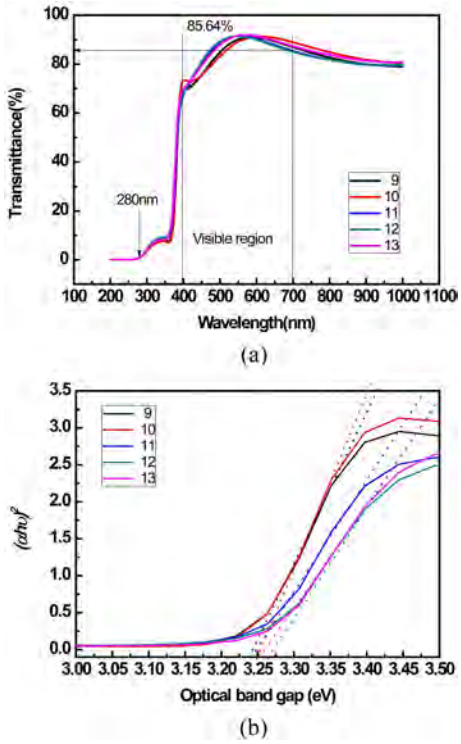

Fig. 3. (a) Transmission of spectra for the ZnO films with the H_2 and O_2 gas flow rates (b) Relationship between absorption coefficient as a function of photon energy. Sample condition refers Table 2.

where $h\nu$ is the photon energy, E_g is the optical band gap, and D is a constant. For a direct transition, $n = 1/2$ or 2/3 and the former value was known to be more suitable for ZnO thin films since it gives the best linear curve in the band-edge region [20, 23]. In Fig. 3(b), the relationship between $(\alpha h\nu)^2$ and $h\nu$ is plotted. The E_g value can be obtained by extrapolating the linear portion to the photon energy axis in that figure. The optical band-gap values obtained for the ZnO thin films deposited with various H_2 and O_2 gas flow rates are summarized in Table 2 and Table 3, respectively.

The optical band gap varied from 3.23 to 3.26 eV with the H_2 gas flow rate change. In case of O_2 gas flow rate change, the optical band gap showed variation of the range of 3.22 ~ 3.24 eV. The band gap values of the synthesized ZnO thin films were lower than the

Table 2. Estimated optical band gap of ZnO films at various H_2 gas flow rate.

	H_2 and O_2 gas flow rate	Estimated optical band gap		Grain Size of (002)Plane		XRD Intensity	
		without annealing	with annealing	without annealing	with annealing	without annealing	with annealing
9	H_2 0.2, O_2 0.4 sccm	3.23	3.23	16.20	15.37	1232	1752
10	H_2 0.4, O_2 0.4 sccm	3.24	3.22	16.32	17.68	1234	1096
11	H_2 0.6, O_2 0.4 sccm	3.24	3.23	15.59	18.09	1430	984
12	H_2 0.8, O_2 0.4 sccm	3.26	3.24	17.19	17.13	1168	1530
13	$H_2$1.0, O_2 0.4 sccm	3.25	3.24	17.65	16.77	1070	1280

Table 3. Estimated optical band gap of ZnO films at various O_2 gas flow rate.

	H_2 and O_2 gas flow rate	Estimated optical band gap		Grain Size of (002) Plane		XRD Intensity	
		without annealing	with annealing	without annealing	with annealing	without annealing	with annealing
14	H_2 0.2, O_2 0.2 sccm	3.23	3.21	16.20	15.37	1158	1016
9	H_2 0.2, O_2 0.4 sccm	3.24	3.23	15.45	15.45	1234	1096
15	H_2 0.2, O_2 0.6 sccm	3.22	3.22	16.14	15.99	991	1054
16	H_2 0.2, O_2 0.7 sccm	3.23	3.23	15.90	16.70	1234	794
17	H_2 0.2, O_2 0.8 sccm	3.23	3.23	15.99	16.92	1196	867
18	$H_2$0.2, O_2 1.0 sccm	3.23	3.23	17.19	16.48	1098	1182

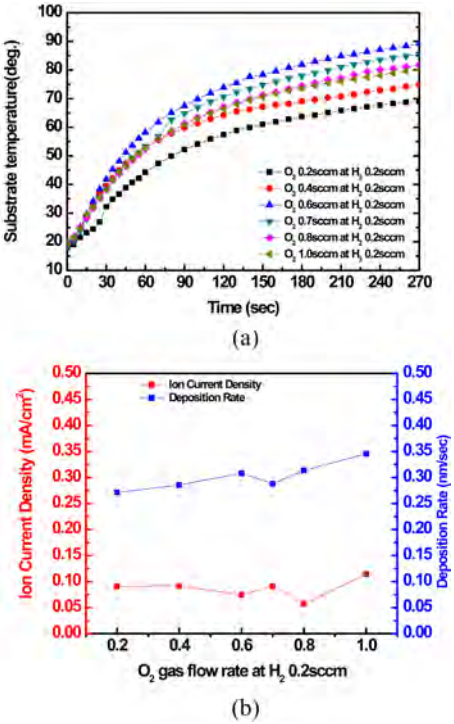

Fig. 4. (a) Temporal change of substrate temperatures and (b) Ion current density, deposition rate and grain size with O_2 gas flow rates change.

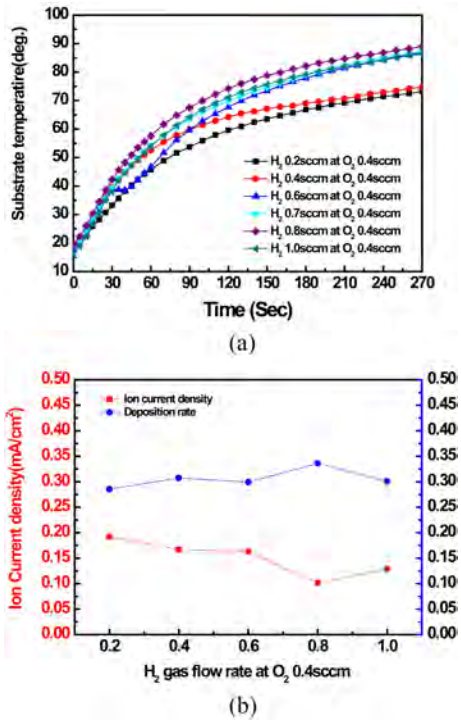

Fig. 5. (a) Temporal change of substrate temperatures and (b) Ion current density, deposition rate and grain size with H_2 gas flow rates change.

band gap of ZnO (3.36 eV) in the literature. It seemed that there was no relation between the optical band gap values and XRD intensity of the deposited ZnO thin film with small change of H_2 and O_2 gas flow rate.

Structural properties of ZnO thin films

With the O_2 flow rates, the temporal change of substrate temperature was shown in Fig. 4(a). The substrate temperature increased from the initial room temperature to 69.1 ~ 89.2 ºC at deposition time of 4 min 30 sec according to O_2 flow rates. The amount of change in the substrate temperature during the deposition was 51.3 ~ 70.3 ºC. Fig. 4(b) shows that the ion current density did not change much with increases in O_2 gas flow rate. The deposition rate was 0.271 ~ 0.345 nm/sec which was higher than the case of deposition at upper substrate position [25].

With changes in H_2 flow rate, the substrate temperature changed from the initial room temperature to 73.2 ~ 89 ºC at deposition time of 4 min 30 sec, as shown in Fig. 5(a). The amount of change in the substrate temperature was 54.7 ~ 70.3 ºC during the deposition time. As can be seen in Fig. 5(b), the ion current density decreased with increase of H_2 gas flow rate. And according to the H_2 flow rate change, the deposition was in the range of 0.285 ~ 0.335 nm/sec which was higher than the case of deposition at upper substrate position [25].

Just after deposition and after annealing of the ZnO thin films, X-ray diffraction (XRD) patterns were measured as shown in Fig. 6(a) and Fig. 7(a) according to O_2 and H_2 flow rates, respectively. The ZnO thin films deposited at the various conditions were polycrystalline with hexagonal structure. The peak positioned at 2θ ≈

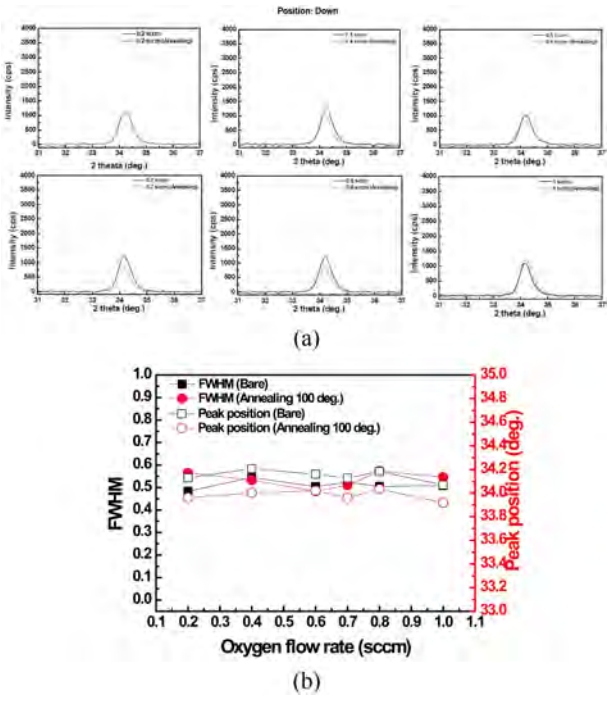

Fig. 6. (a) XRD intensity of ZnO thin film deposited according to O_2 gas flow rates with and without annealing treatment. (b) Change of FWHM and peak position of ZnO thin film with O_2 gas flow rates in condition without and with annealing treatment.

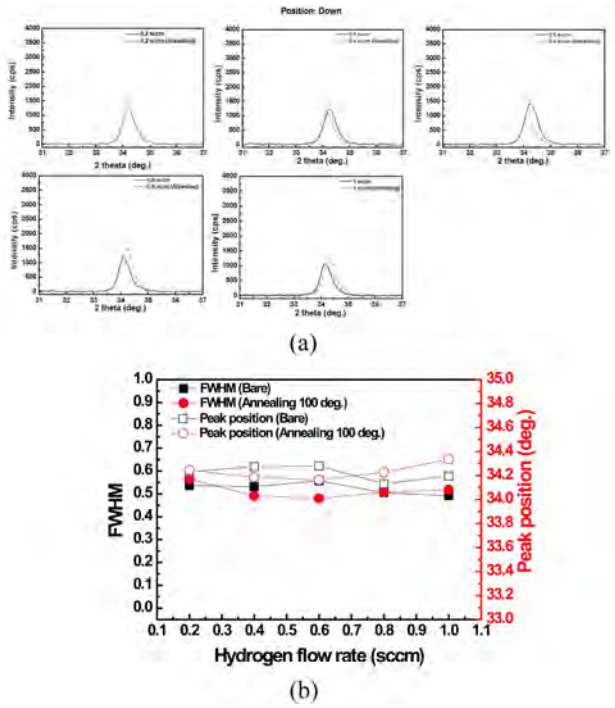

Fig. 7. (a) XRD intensity of ZnO thin film deposited according to H_2 gas flow rates with and without annealing treatment. (b) Change of FWHM and peak position of ZnO thin film with H_2 gas flow rate in condition without and with annealing treatment.

34.14 ° ~ 34.22 ° without annealing and 2θ ≈ 33.98 ° ~ 34.23 ° with annealing corresponding to the (002) ZnO thin film were observed for all samples.

It was possible to obtain 2θ peak position values which was close to 34.4 ° for single crystal of ZnO thin film. It could be attributed to the merit of low thermal damage in FTS system due to the confining magnetic field which decreased flux of high energy ions impinging on the ZnO thin films.

Figs. 6(a) and 7(a) showed that the (002) reflections were the dominant planes for ZnO thin films deposited with change of H_2 and O_2 gas flow rates, respectively. This indicates oriented film growth with the crystallographic c-axes perpendicular to the substrate surface. According to Fig. 6(a) and Fig. 7(a), XRD intensity changed slightly with O_2 and H_2 flow rates, with and without annealing treatment. Fig. 6(b) and Fig. 7(b) show analysis results of the XRD graph, the FWHM and the peak position according to H_2 and O_2 gas flow rates, respectively. The range of FWHM values for all samples was 0.480 ~ 0.565. The lowest FWHM 0.480 was obtained at 0.6sccm H_2 gas flow rates and 0.4 sccm O_2 gas flow rates with annealing treatment in Fig. 7(b). The broadened peak indicates defect sites such as an oxygen vacancies or interstitial zinc in the lattice. The ZnO thin film deposited at 0.2 sccm H_2 gas flow rates and 0.4 sccm O_2 gas flow rates with annealing treatment showed the highest (002) peak shift in Fig. 7(b).

From XRD results, the grain size was calculated by Scherrer's formula, $t = k\lambda/(B\cos\theta)$, k is a constant taken as 1, λ is the X-ray wavelength (CuKα = 0.154 nm), B is the full width at half maximum (FWHM), θ is the Bragg diffraction angle [24].

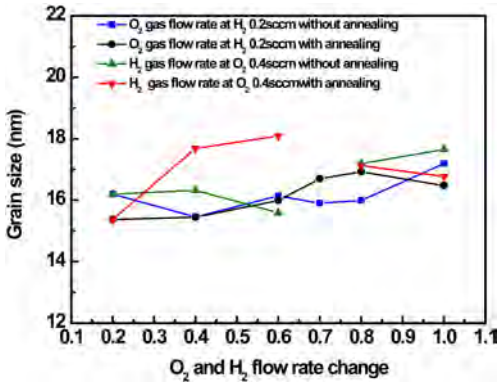

Fig. 8. Grain size with O_2 and H_2 gas flow rates and with and without annealing treatment.

The grain size of the ZnO thin films ranges from 15 nm to 19 nm for crystallographic plane (002) as shown in Table 2 and Table 3 with various H_2 and O_2 flow rates, respectively. Fig. 8 shows the change in grain size according to O_2 and H_2 gas flow rate change and with and without annealing treatment. The grain size and XRD intensity did not change monotonically with H_2 and O_2 gas flow rate.

From these results, the structural properties of the ZnO thin films deposited were not changed much with the flow rates of H_2 and O_2 gases.

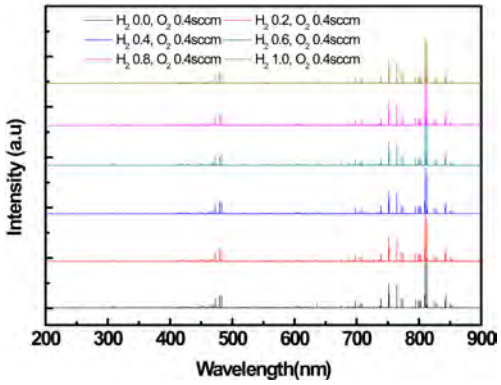

Fig. 9. Full spectrum of $Ar/H_2/O_2$ plasma formed in FTS system. Change of emission intensities with O_2 and H_2 gas flow.

Emission spectroscopy

ZnO thin film synthesis in FTS system is characterized by the bombardment of the growing film with species from the sputtering target and from the plasma. The incident atoms with energies in the eV range—mostly Ar ions from the plasma and neutral atoms reflected at the target—hit the growing film. The properties of the ZnO thin films vary depending on the energy of these species and on the ion-to-neutral ratio [18]. So, the investigation of plasma characteristics would be helpful to understand the change of film properties. To examine the plasma status change, OES was performed at the whole conditions for the ZnO thin film deposition.

Fig. 9 shows OES spectra in the range of 200 nm ~ 900 nm with the change of H_2 gas flow rates. The overall spectrum did not change with the H_2 and O_2 gas flow rates. It could be attributed to the small change of H_2 and O_2 gas flow rates which did not affect the plasma characteristics. From these results, it could be considered that the plasma status was not affected by the small change of H_2 and O_2 flow rates.

Conclusions

ZnO thin film was synthesized by the low processing temperature FTS system with H_2 and O_2 gas flow rate changes. To investigate the plasma characteristics, ion current density and substrate temperature changes were monitored, and OES diagnostics were performed. The overall OES spectrum did not change with the H_2 and O_2 gas flow rates. From the OES analysis results, it could be observed that the plasma status was not affected by small changes of H_2 and O_2 flow rates.

In the analysis of the optical property, the optical band gap values decreased from the conventional value (3.36 eV). But the optical band gap showed little change with the small change of H_2 and O_2 gas flow rates. According to the structural property analysis, the grain size and crystallization were not changed much neither.

However, the electrical properties such as sheet resistance changed dramatically with the small change of H_2 and O_2 gas flow rates. So, the changes in the electrical properties of ZnO thin films could be considered to be a result of changes in chemical composition of the thin films rather than the plasma status. From the results, H_2 and O_2 flow rates can be suggested to effectively control the electrical properties of ZnO thin films.

Acknowledgment

This study was supported by the Global Development Research Center (GDRC) for program of the Korea Institute for Advancement of Technology (KIAT), which is being funded by the Ministry of Trade, Industry & Energy (MOTIE, Grant No. N0000590). We appreciate the help of Dr. Yongjin Kim and Dr. Sang-hun Nam who discussed on the analysis of plasma status and optical properties.

References

1. S.P.S. Arya, O.N. Srivastava, Cryst. Res. Technol. 23 (1988) 669.
2. J.K. Srivastava, L. Agrawal, B. Bhattacharyya, J. Electrochem. Soc. 11 (1989) 3414.
3. Z.C. Jin, C.G. Granqvist, Proc. SPIE 21 (1987) 827.
4. C. Lee, K. Lim, J. Song, Sol. Energy Mater. Sol. Cells 43 (1996) 37.
5. S.J. Pearton, D.P. Norton, K. Ip, Y.W. Heo, T. Steiner, Prog. Mater. Sci. 50 (2005) 293.
6. H.S. Bae, S. Im, Thin Solid Films 469 (2004) 75.
7. S.K. Hazra, S. Basu, Solid State Electron. 49 (2005) 1158.
8. S. Muthukumar, C.R. Gorla, N.W. Emanetoglu, S. Liang, Y. Lu, J. Cryst.Growth 225 (2001) 197.
9. V. Assuncao, E. Fortunato, A. Marques, H. Aguas, I. Ferreira, M.E.V. Costa, R. Martins, Thin Solid Films 427 (2003) 401.
10. S. Jager, B. Szyszka, J. Szczyrbowski, G. Bauer, Surf. Coat. Technol. 98 (1998) 1304.
11. F. Michelotti, A.Belardini, A. Rousseau, A. Ratsimihety, G. Schoer and J. Mueller, J. Non-Cryst, Solids 352 (2006) 2339.
12. H.Guo, J Zhou and Z. Lin, Electrochem. Commun. 10 (2008) 146.
13. M.H. Wang. C. Yao and N.F. Zhang, J. Matter, Process. Technol, 202 (2008) 406.
14. S.Y. Lee, A. Umar, D.I. Suh, J.E. Park, Y.B. Hanhn, J.Y. Ahn and S.K. Lee, Physica E 40 (2008) 866.
15. A. Belaidi, Y. Dittrich, D. Kieven, J. Tornow, K. Schwarzburg, M .Kunst, N. Allsop, M.C. Lux-Steiner and S. Garvrlov, Sol. Energy Mater. Sol. Cells 93 (2009) 1033.
16. A. Janotti and C.G Van de Walle, Rep. Prog. Phys. 72 (2009) 126501.
17. J. Musil, S. Kadlec, and W.-D. Munz, J. Vac. Sci. Technol. A9 (1991) 1171.
18. J.G. Han, J. Phys. D: Appl. Phys. 42 (2009) 043001.
19. M. Gaillard, N. Britun, Y.M. Kim and J.G. Han, J. Phys. D: Appl. Phys. 40 (2007) 809-817.
20. S.T. Tan, B.J. Chen, X.W. Sun, W.J. Fan, H.S. Kwok, X.H. Zhang and S.J. Chua, J. Appl. Phys. 98 (2005) 013505.
21. E.A. Davis, N.F. Mott, Philosophical Mgazine 22 (1970) 903.
22. Y. Kayanuma, Phys. Rev. B 38 (1988) 9797.
23. P. Singh, A. Kumar, Deepak and D. Kaur, Opt. Mater. 30 (2008) 1316.
24. H.R. Kim, S.B. Jin, L. Wen, Y.S. Choi, I.S. Choi, J.G. Han, Journal of Nanoscience and Nanotechnology (submitted).